Earth and Planetary Science Letters 274 (2008) 151–156

Contents lists available at ScienceDirect

Earth and Planetary Science Letters

journal homepage: www.elsevier.com/locate/epsl

An ice core perspective on the age of the Matuyama–Brunhes boundary

G.B. Dreyfus [a,b,*], G.M. Raisbeck [c], F. Parrenin [d], J. Jouzel [a], Y. Guyodo [a], S. Nomade [a], A. Mazaud [a]

[a] Laboratoire des Sciences du Climat et de l'Environnement/Institut Pierre Simon Laplace, CEA-CNRS-UVSQ, CE Saclay, 91191 Gif-sur-Yvette, France
[b] Department of Geosciences, Princeton University, Princeton, New Jersey 08540, USA
[c] Centre de Spectrométrie Nucléaire et de Spectrométrie de Masse, IN2P3-CNRS-Université de Paris-Sud, Bât. 108, 91405 Orsay, France
[d] Laboratoire de Glaciologie et Géophysique de l'Environnement, CNRS-UJF, 38402 St Martin d'Hères, France

A R T I C L E I N F O

Article history:
Received 22 April 2008
Accepted 9 July 2008
Available online 16 July 2008

Editor: R.W. Carlson

Keywords:
age of Matuyama–Brunhes boundary
enhanced Be-10 deposition
Antarctic ice, paleomagnetism

A B S T R A C T

Two intervals of enhanced ^{10}Be flux thought to be associated with periods of low dipole intensity and identified as the Matuyama–Brunhes transition and a precursor event have been observed in the bottom section of the EPICA Dome C ice core [Raisbeck, G.M., Yiou, F., Cattani, O., Jouzel, J., 2006. ^{10}Be evidence for the Matuyama–Brunhes geomagnetic reversal in the EPICA Dome C ice core, Nature 444, 82–84, doi:10.1038/nature05266]. The peaks span 764–776 ka and 788–798 ka on the new EDC3 chronology with a stated absolute age uncertainty of 6 ka (2σ). This chronology uses orbital tuning of atmospheric oxygen-18 ($\delta^{18}O_{atm}$) to correct for anomalies in ice flow in the bottom 500 m of the core. An additional 28 $\delta^{18}O_{atm}$ data points have been measured to improve resolution and verify the accuracy of the tuning and the stated timescale uncertainty. Both the dating of the increased ^{10}Be, and that relative to climatic records, are compared to paleointensity records found in orbitally tuned marine sediments. The mid-point of the ^{10}Be peak associated with the M-B is approximately 10 ka younger than the age determined radioisotopically from lavas with transitional orientations, taking into account recent revisions to the ^{40}Ar/^{39}Ar dating standard and improved precision. Climatic constraints on the EDC3 agescale make an error of this magnitude in the ice chronology implausible. This age difference, however, is consistent with recent modeling suggesting that directional changes are spatially asynchronous, and may precede the dipole intensity minimum in some locations. Although formally less precise than the published age from astrochronologically dated marine sediments, ice core ages are potentially more accurate because they are not subject to lock-in depth uncertainties.

1. Introduction

The Matuyama–Brunhes boundary (M–B) is the most recent geomagnetic polarity reversal, and has been intensively studied in marine and loess sediments and in volcanic rocks (e.g. synthesis study by Love and Mazaud, 1997; lava flow review by Singer et al., 2005). Marine sediments contain magnetic grains that orient themselves in the direction of the magnetic field prevailing at the time of deposition with a relative efficiency that depends on field intensity. As a result marine sediments can provide continuous records of geomagnetic field paleodirection and relative paleointensity. In addition to field direction, volcanic rocks provide discontinuous records of absolute intensity based on thermoremanent magnetization acquired during cooling of the magnetic grains below their Curie and blocking temperatures. Some marine records have indicated that the boundary between the Brunhes and Matuyama chrons had a complex structure, with the polarity reversal being preceded 15 thousand years (ka) earlier by a decrease in paleointensity associated in several cores with a change in direction to normal polarity (Kent and Schneider, 1995; Hartl and Tauxe, 1996). Recent improvements in the analytical precision of the ^{40}Ar/^{39}Ar dating method made it possible to distinguish the age of the M–B transition in Maui lavas at 775.6±1.9 (2σ analytical) (Coe et al., 2004) from a precursor event recorded at 791.7±3.0 ka in Chile (Brown et al., 2004) and at 798.4±6.2 ka in the Canary Islands (Singer et al., 2002). A review of M–B age lavas provided statistical support for the existence of two periods of transitional field orientation separated by ~18 ka (Singer et al., 2005). While improved radioisotopic dating techniques have reduced analytical uncertainties, until recently a 2% uncertainty on the ^{40}K decay constants (Min et al., 2000) limited the precision of the ^{40}Ar/^{39}Ar dating method to about ±16 ka for M–B age volcanic rocks. A new study reduces this uncertainty to 0.31% by dating the Fish Canyon sanidine (FCs) standard using an orbital tuning method (Kuiper et al., 2008)[1]. Furthermore, this study found that the FCs age was too young, and suggested that it be revised older by 0.646% (Kuiper et al., 2008).

The European Project for Ice Coring in Antarctica (EPICA) recently recovered the 3260-meter Dome C (EDC) ice core providing access to

* Corresponding author. Department of Geosciences, Princeton University, Princeton, New Jersey 08540, USA. Tel.: +1 609 375 5448; fax: +1 609 258 1274.
E-mail address: gdreyfus@princeton.edu (G.B. Dreyfus).

[1] A review of the supporting online material for Kuiper et al. (2008) indicates that the 2σ uncertainty should be 0.31% and 0.62% for a ±10 ka and ±20 ka uncertainty in the astronomical age, respectively, not 0.25% as stated in the abstract.

0012-821X/$ – see front matter
doi:10.1016/j.epsl.2008.07.008

800 ka of climate history (EPICA community members, 2004; Jouzel et al., 2007). A depth interval with enhanced ^{10}Be flux close to the bottom of the core has been interpreted as recording the M–B (Raisbeck et al., 2006). Global production of ^{10}Be is inversely proportional to approximately the square root of the magnetic field intensity (Lal and Peters, 1967), so that increased flux is expected to be associated with decreased paleointensity. This effect is weakest poleward of approximately 60° latitude (Masarik and Beer, 1999) because shielding by the dipole field is weak at high latitudes. While the latitudinal origin and transport processes are not fully understood, excess ^{10}Be deposition in the polar regions at times of reduced field intensity have been observed in association with the Laschamp excursion in Greenland (Yiou et al., 1997; Beer et al., 1992) and Antarctica (Raisbeck et al., 1987; Raisbeck et al., 2007).

The EDC record allows, for the first time, the temporal evolution of the geomagnetic dipole intensity to be investigated using a chronology constrained by modeling ice flow and orbitally tuning the δ^{18}O of O_2 in trapped air. In principle, physical constraints on accumulation rate and ice sheet thinning result in ice core records providing more accurate information on the duration of events than other sedimentary records. The paleomagnetic record in marine sediments is also subject to acquisition processes that can result in the signal being smoothed and shifted where an excursion or inversion is recorded (e.g. Mazaud, 1996; Roberts and Winklhofer, 2004). As a result, stacks of many records are required for accurate reconstructions of event durations (e.g. Valet et al., 2005), but at the cost of reduced temporal resolution.

Here we compare the ^{10}Be flux profile from the EDC ice core with paleointensity records covering the M–B from marine sediments. In addition to these paleomagnetic parameters, both archives contain climate records, which we compare to distinguish between differences in the recorded field behavior and discrepancies due to differences in timescales. The ages of increased ^{10}Be flux and intensity minima are then compared with the radioisotopically dated lava record.

2. Methods: the EDC3 chronology

The basic chronology of ice cores at low-accumulation sites such as EDC comes from glaciological models that convert depth to age taking into consideration net accumulation and flow of the ice. The EDC chronology used here (named EDC3) uses such an approach. It adopts an inverse method to constrain poorly known accumulation and flow model parameters using chronological age markers with Gaussian uncertainty windows (Parrenin et al., 2007a,b). This timescale presents several important improvements over the previous EPICA Dome C chronology (EDC2) (EPICA community members, 2004), in part by using a more extensive set of chronological markers derived from parameters in the ice core.

The bottom 500 m of the ice sheet is critical to us because it includes the ^{10}Be peaks thought to represent the M–B transition. Comparison with other records indicates that the stratigraphy is intact to the bottom of the core (Dreyfus et al., 2007). The EDC3 chronology corrects for variations in ice thinning rate in the bottom 500 m of the ice sheet potentially due to horizontal stresses not captured by the one dimensional flow model (Dreyfus et al., 2007; Parrenin et al., 2007a). These authors corrected the chronology for these flow anomalies using orbital tuning of the δ^{18}O of atmospheric O_2 (noted $\delta^{18}O_{atm}$ after correction for gravitational fractionation in the firn) extracted from occluded air in the ice. Variations in $\delta^{18}O_{atm}$ have been observed to be coherent with variations in northern hemisphere summertime insolation associated with precession of the Earth's orbit (Jouzel et al., 1996). The tuning used in EDC3 assumes that $\delta^{18}O_{atm}$ tracks the precession parameter with a constant 5000-year phase lag (Shackleton, 2000). This phasing has been shown to vary by up to ±6000 years over the past 360 ka (Kawamura et al., 2007) due to variability in the hydrologic and biospheric cycling of oxygen between seawater and the atmosphere (known as the Dole effect). Dreyfus et al. (2007) adopted a 2σ Gaussian uncertainty of ±6000 years to account for these phase variations in the past. Provided that each precession cycle is correctly identified, the uncertainty in phasing is not cumulative. Rather, it encompasses the range of variability in the hydrologically mediated response of $\delta^{18}O_{atm}$ to a given insolation cycle.

There are three main sources of uncertainty in the chronology derived using this tuning approach: 1) the constant phasing assumption, 2) the tuning target choice, 3) data resolution and tie point identification. The influence of the first two factors has been addressed and found to be within the stated 6 ka uncertainty (Dreyfus et al., 2007). For the third, 28 additional points have been measured between 700 and 800 ka, improving the $\delta^{18}O_{atm}$ resolution from 3371 to 1860 years. These data are shown as empty circles in the top panel of Fig. 1. We have excluded 4 points with $\delta O_2/N_2$ inferior to −25‰ with respect to air on the basis of excessive oxygen depletion. We repeat the tuning using 18 redefined tie points between 3035 m and 3189 m to determine the effect on the chronology. Tie points changed by less than 1.5 m (with 1 m representing between 300 and 1350 years over this interval) in all but 4 cases. Applying the same least-squares fitting algorithm as used in Dreyfus et al. (2007) to the revised tie points yielded a chronology that agreed with EDC3 to within 1200 years over the interval covering the M–B ^{10}Be peaks and within 3500 years over the entire interval. This test adds confidence in the stated ±6 ka uncertainty. A fourth uncertainty arises from the anomalous flow regime in the bottom 500 meters of the core (Dreyfus et al., 2007). The uncertainty on the duration of events shorter than the time between tie points (i.e. <11 ka, half a precession cycle) recorded in this bottom section has been estimated to be on the order of 40% due to the combined instantaneous accumulation rate uncertainty and flow correction (Dreyfus et al., 2007; Parrenin et al., 2007b). New CH_4 and CO_2 records from the EDC core spanning three climatic oscillations between 755 and 773 ka do not show any evidence for additional anomalous flow over this interval (Lüthi et al., 2008; Loulergue et al., 2008).

3. Results and discussion

Enhanced ^{10}Be fluxes were found spanning 3161–3170 m and 3180–3187 m (Raisbeck et al., 2006), corresponding to the age ranges 764–776 ka and 788–798 ka on the EDC3 chronology (Fig. 1). The two ^{10}Be peaks suggest that the M–B is characterized by two distinct periods of reduced geomagnetic dipole intensity separated by about 23 ka. Quantitative discussion of the evolution of the dipole intensity is complicated by several factors. First, while the ^{10}Be production function is known to be inversely related to dipole intensity (Lal and Peters, 1967; Beer et al., 2002), the relationship between production and deposition at high-latitudes is more uncertain. Climate models incorporating ^{10}Be production and transport suggest that ^{10}Be concentration in polar ice may depend on climate driven changes in the precipitation rate (Field et al., 2006). Raisbeck et al. (2006) accounted for the direct influence of precipitation rate by converting ^{10}Be concentration to flux using the snow accumulation rate from the ice core chronology. This has been updated here using revised accumulation rates implied by EDC3. Second, as a result of spikes in the raw ^{10}Be data, the data is reported as median fluxes (Raisbeck et al., 2006).

3.1. Comparison of the EDC ice core ^{10}Be record with marine paleointensity records

The age of the M–B reversal in astronomically tuned marine records has previously been reported as 775±10 ka in an Indian Ocean core (Bassinot et al., 1994) and 778±2 ka in a stacked record (Tauxe et al., 1996). The latter is at the older edge of the ice core age of the ^{10}Be

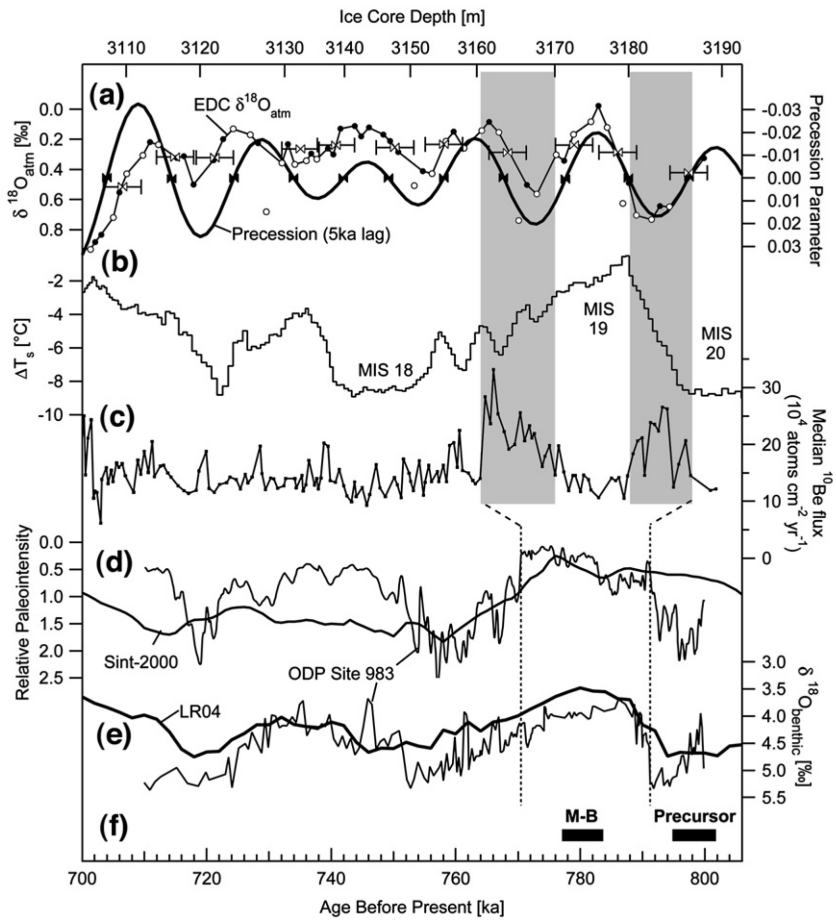

Fig. 1. Paleomagnetic and paleoclimatic records of the Matuyama–Brunhes boundary from the EPICA Dome C (EDC) ice core (a–c), marine sediments (d–e), and lavas (f). Shading highlights the Matuyama–Brunhes reversal (M–B) and "precursor" events as determined from the ^{10}Be enhancement in the ice core record (Raisbeck et al., 2006) (c). Since ^{10}Be production is inversely proportional to field intensity, dotted lines represent a possible correlation between maxima in ^{10}Be flux and minima in normalized paleointensity from ODP 983 (Channell and Kleiven, 2000) and the Sint-2000 paleointensity stack (Valet et al., 2005) (d), plotted here on an inverted relative scale. We account for differences in timescales by comparing the EDC temperature change inferred from the deuterium content of the ice (Jouzel et al., 2007) (b) with the marine benthic $\delta^{18}O$ climate records of ODP 983 (Channell and Kleiven, 2000) and the LR04 stack (Lisiecki and Raymo, 2005) (e). Records in (d) and (e) are on their published timescales. EDC data are shown on the EDC3 timescale (Parrenin et al., 2007b), with depths on top axis, which is derived from a combination of ice flow modeling (Parrenin et al., 2007a) and orbital tuning of atmospheric oxygen ($\delta^{18}O_{atm}$: open circles this study, filled circles (Dreyfus et al., 2007); bow-ties indicate tie-points and 3 ka uncertainty due to phasing assumptions) to the precession parameter (Laskar et al., 2004) (a). The ages of radioisotopically dated lavas containing transitional geomagnetic field orientations are represented by dark bars (2σ) and have been recalculated from Singer et al. (2005, and references therein) using the revisions from Kuiper et al. (2008) (f).

peak believed to correspond to the M–B reversal. In Fig. 1, we compare the EDC record with paleomagnetic and paleoclimatic indicators from the high-resolution North Atlantic ODP 983 marine sediment core (Channell and Kleiven, 2000), the LR04 marine $\delta^{18}O_{benthic}$ stack (Lisiecki and Raymo, 2005), and the Sint-2000 stack of 10 marine paleointensity records (Valet et al., 2005). The $\delta^{18}O_{benthic}$ record of ODP 983 and the EDC temperature profile (Jouzel et al., 2007) both suggest that the M–B reversal occurred after the interglacial maximum of stage 19, during the cooling phase. By contrast, in the widely used composite LR04 $\delta^{18}O_{benthic}$ record, Lisiecki and Raymo (2005) cite a value of 780 ka for the M–B, which would place it at the peak of stage 19 in their timescale. However, if one places the M–B in the same stratigraphic position relative to the climate record as seen in the ice core, this would make its age in better agreement with that seen in the ice core, as well as with that of ODP 983.

The process by which marine sediments acquire their magnetic signal tends to smooth geomagnetic variations and may shift the paleomagnetic record towards older ages relative to climate proxies in the core. Lock-in depth can be limited to a centimeter-scale (Tauxe et al., 1996; Mazaud, 1996); however, larger, decimeter-scale, lock-in depths have also been advocated (e.g., Channell and Guyodo, 2004). We note that ODP 983 records the M–B at a younger age (shallower depth) with respect to the isotope curve than most other marine records (Channell and Kleiven, 2000). This might be because of the relatively high (~13 cm/ka) mean sedimentation rate at Site 983 during the reversal (Channell and Kleiven, 2000). High sedimentation rates may reduce the effect of shifts resulting from magnetization acquisition processes (Roberts and Winklhofer, 2004). Though the authors do not explicitly consider lock-in depth processes, the comparison of the age of the Mono Lake and Laschamp events as dated in the NAPIS-75 paleointensity stack (Laj et al., 2000) of 6 high sedimentation rate North Atlantic records (including ODP 983) with cosmogenic nuclide records in Greenland (Wagner et al., 2000; Wagner et al., 2001) and radioisotopically dated volcanic rocks (Guillou et al., 2004) suggests that any temporal delay due to lock-in processes is minimal for these cores. We note, however, that Tauxe et al. (1996) did not observe a correlation between position of the M–B with respect to stage 19 and sedimentation rate in their study of 19 other marine cores.

Examined in detail, there are small differences in the relative timescales of the different records. Both ODP 983 and LR04 timescales are derived by tuning benthic isotope profiles to orbitally forced ice volume models. As described above, the ice core EDC3 chronology uses $\delta^{18}O$ of atmospheric O_2 tuned to variations in the precession parameter. While related, these tuning targets and oxygen isotope records emphasize different components of the climate system:

response of high-latitude ice sheets to summer insolation in the tuned marine record (Imbrie and Imbrie, 1980), and lower-latitude vegetation and hydrology in the ice core case (Bender et al., 1994; Malaizé et al., 1999). The Sint-2000 stack of Valet et al. (2005) is based on the timescale of ODP 851 (Meynadier et al., 1995). Taking the records on their respective timescales, the ^{10}Be peak begins approximately at the same time as the minimum in intensity recorded at 775 ka in ODP 983 and Sint-2000. In the EDC chronology, the highest median ^{10}Be flux is measured between 764 and 768 ka and occurs 4 to 8 ka after the intensity minimum in both the ODP 983 and stacked paleointensity records. In addition to these differences in timing, the duration of the low paleointensity associated with the M–B recorded in ODP 983 is much longer than the period of elevated ^{10}Be in EDC (it almost encompasses both periods of low field inferred from the two ^{10}Be maxima in the ice core). One possible explanation for the absence of two clear minima in the marine record is that magnetization acquisition processes smoothed the paleointensity signal (Roberts and Winklhofer, 2004) and/or a non-dipole component of the geomagnetic field was present at Site 983. Alternatively, Channell and Kleiven (2000) have suggested that the very narrow intensity drop at ~791 ka in their record might represent the "precursor" event seen in other sedimentary records. The ages of the temperature maximum for stage 19 (at the end of Termination IX) are nearly the same for EDC and ODP 983. However, there is a large difference (5 ka) in the start and duration of the termination. In the ice core the precursor event occurs during Termination IX. In the ODP 983 record, the transition between MIS20 and MIS19 may be condensed. This could explain the narrowness of the decrease in paleointensity at ~791 ka. The Sint-2000 stack does not show a clear intensity minimum prior to the M–B, but several of the source records contain intensity minimum features lost in the stacking (Valet et al., 2005). Hartl and Tauxe (1996) found several marine records with an intensity minimum approximately 15 ka before the M–B reversal.

When comparing the ODP 983 and Sint-2000 paleointensity curves, it is necessary to consider that these records are slightly different in nature. The ODP 983 record is a single record from a specific location and was calibrated assuming that during reversals, the minimum of intensity is of about 7.5 μT (normalized to its mean in Fig. 1). In contrast, the Sint-2000 stack is a compilation of 10 paleointensity records, obtained after normalizing individual records to their measured mean. It is a statistically more robust description of the long-term evolution of the relative dipole strength than individual records. Indeed, individual paleointensity records can be affected to some extent by lithological overprints (e.g., Guyodo et al., 2000), or may have non-dipole components if their mean sedimentation rate is high. Plotted on a relative paleointensity scale, both records are consistent with a M–B surface intensity reduction to ~10–20% of pre- and post-transitional surface intensity (Love and Mazaud, 1997).

3.2. The ice core and lava records

The EDC3 ages for the M–B transition and precursor event, taken at the midpoint of the ^{10}Be peaks are 770±6 ka (2σ) and 793±6 ka, respectively. We recalculate here the ^{40}Ar/^{39}Ar lava age for the M–B using the revised FCs age from Kuiper et al. (2008) and uncertainty of 0.31% (from the supplementary materials, 2 sigma uncertainty assuming ±10 kyr uncertainty in the astronomical tuning gives 0.088/28.201 = 0.31%). Using the 20 individual isochrones from flows 59, 58, 52, 50, 45, and 37 from Coe et al. (2004), we calculate an M–B age from Maui lavas of 780.3±3.4 ka (2σ external; MSWD = 1.4). Including the 5 TN-16 isochrones from La Palma (Singer et al., 2002) yields an M–B lava age of 780.4±3.3 ka (MSWD = 1.3). We have used the individual isochrones rather than the grouped flows, as done by Coe et al. (2004) and Singer et al. (2005), because the MSWD for the grouped flows suggests the observed width of the distribution is dominated by something other than analytical errors. In contrast, the distribution of the individual isochrones taken together is comparable to the analytical uncertainty. We recalculate the age of the precursor from Singer et al. (2005) to be 798.3±3.5 ka.

The ice core age for the midpoint of the M–B ^{10}Be peak is 10 ka younger than the radioisotopically-dated lava age of 780.4±3.3 ka. The midpoint of the older ^{10}Be peak is 5.3 ka younger than the lava age for the precursor, however, this difference is less than the combined EDC3 and ^{40}Ar/^{39}Ar dating uncertainty. The 18±3 ka separating the M–B and precursor measured in the lava record agrees within error with the 23 ±9 ka separation in the ice chronology. This age comparison assumes that transitional orientations of the magnetic field recorded in lavas occur synchronously with the midpoints of the two maxima of ^{10}Be flux deposited over Antarctica. Recent geomagnetic field modeling suggests that transitional orientations at the surface may in fact not be synchronous at all locations, with local directional changes occurring up to 6 ka before the dipole intensity minimum (Leonhardt and Fabian, 2007). We note that this modeling study found that transitional orientations in the central Pacific (80% of the M–B dated lavas are from Maui) preceded the dipole minimum by 6 ka, however, these results depend on the non-dipole terms, which are poorly constrained for this period. Taking the beginning of the younger ^{10}Be peak (776±6 ka) as the onset of the intensity minimum, the age obtained for both Maui and La Palma transitional lavas flows (780.4± 3.3 ka) could correspond to the beginning of the dipole intensity minimum. The climate record does support a shift up to 6 ka older of the tie point at 779 ka. Chronologies based on orbital tuning of the O_2/N_2 ratio for the Vostok (Suwa and Bender, 2008) and Dome Fuji (Kawamura et al., 2007) ice cores indicate that the phase lag between $\delta^{18}O_{atm}$ and the precession forcing tends to be reduced following interglacial maxima. Such a shift would put the start of the ^{10}Be peak closer to 780 ka. The alternative explanation of the EDC3 agescale being too young by 10 ka at the M–B transition is implausible given the constraints of the orbital tuning. Such an age difference would imply the $\delta^{18}O_{atm}$ lagged the insolation forcing by half a precession cycle, which is 4 ka longer than the greatest lag observed over the past 400 ka (Kawamura et al., 2007; Suwa and Bender, 2008). If Dreyfus et al. (2007) skipped or added a precession cycle in their orbital tuning, we would expect an age difference of ±22 ka. An error between 6 ka and 22 ka would require extreme behavior of the climate system, which the authors consider unlikely.

Dipole field strength has been observed to recover rapidly once normal polarity is achieved both in marine sediments (Valet and Meynadier, 1993; Meynadier et al., 1994; Hartl and Tauxe, 1996; Valet et al., 2005) and lavas (Gratton et al., 2007). Therefore the return of ^{10}Be fluxes to normal levels in the EDC core provides a more precise age reference. The sharp reduction in ^{10}Be at 764±6 ka, for example, would suggest rapid increase in field intensity and establishment of normal polarity at this time. This age is consistent with the fully normal Maui lava flow following the M–B with a recalculated age of 760.9±6.4 ka (Coe et al., 2004). For comparison, the return to normal polarity and intensity occurs at ~770 ka in both the ODP 983 (Channell and Kleiven, 2000) and neighboring ODP 984 sediment records (Channell et al., 2004).

4. Conclusion

The median ^{10}Be flux recorded in the EDC ice core and dated with the EDC3 chronology presents an estimate of the age and duration of the paleointensity minimum of the geomagnetic field at the M–B transition and a precursor event constrained by orbital tuning and ice flow modeling. The ice core record has the advantage over marine sedimentary records of no lock-in associated uncertainty. The two paleointensity minima are separated by approximately 20 ka and lasted 10 to 12 ka. We date these periods at 764–776 ka and 788–798 ka with an estimated uncertainty of ±6 ka on the absolute ages and 40% uncertainty on duration. The location of the M–B transition with respect to the end of stage 19 and the occurrence of the precursor over termination IX agree with a broad minimum in the ODP 983 and stacked Sint-2000 paleointensity records, with the precursor possibly correlating with a very narrow intensity minimum found in the sediment record. The difference in age between the radioisotopically determined age of the M–B, based principally on transitionally oriented flows from Maui (Coe et al., 2004), and the ice core age based on enhanced ^{10}Be is unlikely to be due to errors in the ice core dating or the recent revision of the FCs age (Kuiper et al., 2008). Assuming the uncertainties in one or both of the chronologies have not been underestimated, the difference in timing could also be due to asynchrony in some locations between transitional directions and minimal dipole intensity, as suggested by the recent modeling study of Leonhardt and Fabian (2007), in which directional changes in some locations preceded the minimum in dipole intensity. Additional lavas spanning the M–B reversal in other geographical locations would need to be identified and precisely dated to test this idea. If trends suggested by this modeling are correct, then we would argue that the minimum in dipole intensity recorded by the ^{10}Be, not the spatially limited lava record, should be used to define the age of the M–B.

The application of new orbital tuning approaches based on local summer insolation proxies (Raynaud et al., 2007; Kawamura et al., 2007; Suwa, 2007; Suwa and Bender, 2008) may further improve the dating of this bottom section of the EDC ice core, and thus the absolute dating of the Matuyama–Brunhes boundary.

Acknowledgements

We thank B. Minster for help with experimental measurements, and M. Stievenard, S. Falourd and O. Cattani for technical support. We also thank B. Singer for his detailed review, and J.E.T. Channell for providing the ODP 983 paleointensity data. This work is a contribution to the European Project for Ice Coring in Antarctica (EPICA), a joint European Science Foundation/European Commission scientific programme, funded by the EU (EPICA-MIS) and by national contributions from Belgium, Denmark, France, Germany, Italy, the Netherlands, Norway, Sweden, Switzerland and the UK. The main logistic support was provided by IPEV and PNRA (at Dome C) and AWI (at Dronning Maud Land). Additional funding was provided by the French Agence Nationale de la Recherche (PICC project). This is EPICA publication no. 207 and LSCE contribution no. 3128.

References

Bassinot, F.C., Labeyrie, L.D., Vincent, E., Quidelleur, X., Shackleton, N.J., Lancelot, Y., 1994. The astronomical theory of climate and the age of the Brunhes–Matuyama magnetic reversal. Earth Planet. Sci. Lett. 126, 91–108.

Beer, J., Johnsen, S.J., Bonani, G., Finkel, R.C., Langway, C.C., Oeschger, H., Stauffer, B., Suter, M., Wölfli, W., 1992. ^{10}Be peaks as time markers in polar ice core records. In: Bard, E., Broecker, W.S. (Eds.), The Last Deglaciation: Absolute and Radiocarbon Chronologies. Springer, New York, pp. 141–143.

Beer, J., Muscheler, R., Wagner, G., Laj, C., Kissel, C., Kubik, P.W., Synal, H.-A., 2002. Cosmogenic nuclides during Isotope Stages 2 and 3. Quat. Sci. Rev. 21, 1129–1139.

Bender, M., Sowers, T., Labeyrie, L., 1994. The Dole effect and its variations during the last 130,000 years as measured in the Vostok ice core. Global Biogeochem. Cycles 8 (3), 363–376.

Brown, L.L., Singer, B.S., Pickens, J.C., Jicha, B.R., 2004. Paleomagnetic directions and ^{40}Ar/^{39}Ar ages from the Tatara-San Pedro volcanic complex, Chilean Andes: lava record of a Matuyama–Brunhes precursor? J. Geophys. Res. 109, B12101.

Channell, J.E.T., Kleiven, H.F., 2000. Geomagnetic palaeointensities and astrochronological ages for the Matuyama–Brunhes boundary and the boundaries of the Jaramillo Subchron: palaeomagnetic and oxygen isotope records from ODP Site 983. Phil. Trans. R. Soc. Lond. A 358, 1027–1047.

Channell, J.E.T., Guyodo, Y., 2004. The Matuyama Chronozone at ODP 982 (Rockall Bank): evidence for decimeter-scale magnetization lock-in depths. In: Channell, J.E.T., Kent, D.V., Lowrie, W., Meert, J.G. (Eds.), Timescales of the Paleomagnetic Field. Geophysical Monograph Series, vol. 145, doi:10.1029/145GM15.

Channell, J.E.T., Curtis, J.H., Flower, B.P., 2004. The Matuyama–Brunhes boundary interval (500–900 ka) in North Atlantic drift sediments. Geophys. J. Int. 158, 489–505.

Coe, R.S., Singer, B.S., Pringle, M.S., Zhao, X., 2004. Matuyama–Brunhes reversal and Kamikatsura event on Maui: paleomagnetic directions, ^{40}Ar/^{39}Ar ages and implications. Earth Planet. Sci. Lett. 222, 667–684.

Dreyfus, G., Parrenin, F., Lemieux-Dudon, B., Durand, G., Masson-Delmotte, V., Jouzel, J., Barnola, J.M., Panno, L., Spahni, R., Tisserand, A., Siegenthaler, U., Leuenberger, M., 2007. Anomalous flow below 2700 m in the EPICA Dome C ice core detected using δ^{18}O of atmospheric oxygen measurements. Clim. Past 3, 341–353.

EPICA community members, 2004. 8 Glacial cycles from an Antarctic ice core. Nature 429, 623–628.

Field, C.V., Schmidt, G.A., Koch, D., Salyk, C., 2006. Modeling production and climate-related impacts on ^{10}Be concentration in ice cores. J. Geophys. Res. 111, doi:10.1029/2005JD006410.

Gratton, M.N., Shaw, J., Brown, L.L., 2007. Absolute palaeointensity variation during a precursor to the Matuyama–Brunhes transition recorded in Chilean lavas. Phys. Earth Planet. Inter. 162, 61–72.

Guillou, H., Singer, B.S., Laj, C., Kissel, C., Scaillet, S., Jicha, B.R., 2004. On the age of the Laschamp geomagnetic excursion. Earth Planet. Sci. Lett. 227, 331–343.

Guyodo, Y., Gaillot, P., Channell, J.E.T., 2000. Wavelet analysis of relative geomagnetic paleointensity at ODP Site 983. Earth Planet. Sci. Lett. 184, 109–123.

Hartl, P., Tauxe, L., 1996. A precursor to the Matuyama/Brunhes transition-field instability as recorded in pelagic sediments. Earth Planet. Sci. Lett. 138, 121–135.

Imbrie, J., Imbrie, J.Z., 1980. Modeling the climatic response to orbital variations. Science 207, 943–953, doi:10.1126/science.207.4434.943.

Jouzel, J., Waelbroeck, C., Malaize, B., Bender, M., Petit, J.R., Stievenard, M., Barkov, N.I., Barnola, J.M., King, T., Kotlyakov, V.M., Lipenkov, V., Lorius, C., Raynaud, D., Ritz, C., Sowers, T., 1996. Climatic interpretation of the recently extended Vostok ice records. Clim. Dyn. 12, 513–521.

Jouzel, J., Masson-Delmotte, V., Cattani, O., Dreyfus, G., Falourd, S., Hoffmann, G., Nouet, J., Barnola, J.M., Chappellaz, J., Fischer, H., Gallet, J.C., Johnsen, S., Leuenberger, M., Loulergue, L., Luethi, D., Oerter, H., Parrenin, F., Raisbeck, G.M., Raynaud, D., Schwander, J., Spahni, R., Souchez, R., Selmo, E., Schilt, A., Steffensen, J.P., Stenni, B., Stauffer, B., Stocker, T.F., Tison, J.L., Werner, M., Wolff, E.W., 2007. Orbital and millennial Antarctic climate variability over the last 800,000 years. Science 317, 793.

Kawamura, K., Parrenin, F., Lisiecki, L., Uemura, R., Vimeux, F., Severinghaus, J.P., Hutterli, M.A., Nakazawa, T., Aoki, S., Jouzel, J., Raymo, M.E., Matsumoto, K., Nakata, H., Motoyama, H., Fujita, S., Goto-Azuma, K., Fujii, Y., Watanabe, O., 2007. Northern Hemisphere forcing of climatic cycles in Antarctica over the past 360,000 years. Nature 448 (7156), 912–916.

Kent, D.V., Schneider, D.A., 1995. Correlation of paleointensity variation records in the Brunhes/Matuyama polarity transition interval. Earth Planet. Sci. Lett. 129, 135–144.

Kuiper, K.F., Deino, A., Hilgen, F.J., Krijgsman, W., Renne, P.R., Wijbrans, J.R., 2008. Synchronizing rock clocks of Earth history. Science 320, 500–504, doi:10.1126/science.1154339.

Laj, C., Kissel, C., Mazaud, A., Channell, J.E.T., Beer, J., 2000. North Atlantic palaeointensity stack since 75 ka (NAPIS-75) and the duration of the Laschamp event. Phil. Trans. R. Soc. Lond. A 358, 1009–1025.

Lal, D., Peters, B., 1967. Cosmic ray produced radioactivity on the Earth. In: Fluegge, S., Sitte, K. (Eds.), Handbuch der Physik. Springer-Verlag, Berlin, pp. 551–612.

Laskar, J., Robutel, P., Joutel, F., Gastineau, M., Correia, A.C.M., Levrard, B., 2004. A long-term numerical solution for the insolation quantities of the Earth. A&A 428, 261–285.

Leonhardt, R., Fabian, K., 2007. Paleomagnetic reconstruction of the global geomagnetic field evolution during the Matuyama/Brunhes transition: iterative Bayesian inversion and independent verification. Earth Planet. Sci. Lett. 253, 172–195.

Lisiecki, L.E., Raymo, M.E., 2005. A Pliocene–Pleistocene stack of 57 globally distributed benthic δ^{18}O records. Paleoceanography 20, PA1003, doi:10.1029/2004PA001071.

Loulergue, L., Schilt, A., Spahni, R., Masson-Delmotte, V., Blunier, T., Lemieux, B., Barnola, J.-M., Raynaud, D., Stocker, T.F., Chappellaz, J., 2008. Orbital and millennial-scale features of atmospheric CH_4 over the past 800,000 years. Nature 453, 383–386.

Love, J.J., Mazaud, A., 1997. A database for the Matuyama–Brunhes magnetic reversal. Phys. Earth Planet. Inter. 103, 207–245.

Lüthi, D., Le Floch, M., Bereiter, B., Blunier, T., Barnola, J.M., Siegenthaler, U., Raynaud, D., Jouzel, J., Fischer, H., Kawamura, K., Stocker, T.F., 2008. High resolution carbon dioxide concentration record 650,000–800,000 years before present. Nature 453, 379–382.

Malaizé, B., Paillard, D., Jouzel, J., Raynaud, D., 1999. The Dole effect over the last two glacial-interglacial cycles. J. Geophys. Res. 104 (D12), 14199–14208.

Masarik, J., Beer, J., 1999. Simulation of particle fluxes and cosmogenic nuclide production in the Earth's atmosphere. J. Geophys. Res. 104, 12099–12111.

Mazaud, A., 1996. 'Sawtooth' variation in magnetic intensity profiles and delayed acquisition of magnetization in deep sea cores. Earth Planet. Sci. Lett. 139, 379–386.

Meynadier, L., Valet, J.-P., Bassinot, F.C., Shackleton, N.J., Guyodo, Y., 1994. Asymmetrical saw-tooth pattern of the geomagnetic field intensity from equatorial sediments in the Pacific and Indian Oceans. Earth Planet. Sci. Lett. 126, 109–127.

Meynadier, L., Valet, J.-P., Shackleton, N.J., 1995. Relative geomagnetic intensity during the last 4 M.Y. from the equatorial Pacific. In: Pisias, N.G., Mayer, L.A., Janecek, T.R., Palmer-Julson, A., van Andel, T.H. (Eds.), Proceedings of the Ocean Drilling Program. Scientific Results, vol. 138. College Station, Tx, pp. 779–795.

Min, K., Mundil, R., Renne, P.R., Ludwig, K., 2000. A test for systematic errors in ^{40}Ar/^{39}Ar geochronology through comparison with U/Pb analysis of a 1.1 Ga rhyolite. Geochim. Cosmochim. Acta 64, 78–98.

Parrenin, F., Dreyfus, G., Durand, G., Fujita, S., Gagliardini, O., Gillet, F., Jouzel, J., Kawamura, K., Lhomme, N., Masson-Delmotte, V., Ritz, C., Schwander, J., Shoji, H., Uemura, R., Watanabe, O., Yoshida, N., 2007a. 1-D-ice flow modelling at EPICA Dome C and Dome Fuji, East Antarctica. Clim. Past 3, 243–259.

Parrenin, F., Barnola, J.-M., Beer, J., Blunier, T., Castellano, E., Chappellaz, J., Dreyfus, G., Fischer, H., Fujita, S., Jouzel, J., Kawamura, K., Lemieux-Dudon, B., Loulergue, L., Masson-Delmotte, V., Narcisi, B., Petit, J.R., Raisbeck, G., Raynaud, D., Ruth, U., Schwander, J., Severi, M., Spahni, R., Steffensen, J.P., Svensson, A., Udisti, R., Waelbroeck, C., Wolff, E.W., 2007b. The EDC3 chronology for the EPICA Dome C ice core. Clim. Past 3, 485–497.

Raisbeck, G.M., Yiou, F., Bourlès, D., Lorius, C., Jouzel, J., Barkov, N.I., 1987. Evidence for two intervals of enhanced Be-10 deposition in Antarctic ice during the last glacial period. Nature 326, 273–277.

Raisbeck, G.M., Yiou, F., Cattani, O., Jouzel, J., 2006. ^{10}Be evidence for the Matuyama–Brunhes geomagnetic reversal in the EPICA Dome C ice core. Nature 444, 82–84, doi:10.1038/nature05266.

Raisbeck, G.M., Yiou, F., Jouzel, J., Stocker, T.F., 2007. Direct north-south synchronization of abrupt climate change record in ice cores using Beryllium 10. Clim. Past 3, 541–547.

Raynaud, D., Lipenkov, V., Lemieux-Dudon, B., Duval, P., Loutre, M.-F., Lhomme, N., 2007. The local insolation signature of air content in Antarctic ice. A new step toward an absolute dating of ice records. Earth Planet. Sci. Lett. 261, 337–349, doi:10.1016/j.epsl.2007.06.025.

Roberts, A.P., Winklhofer, M., 2004. Why are geomagnetic excursions not always recorded in sediments? Constraints from post-depositional remanent magnetization lock-in modelling. Earth Planet. Sci. Lett. 227, 345–359, doi:10.1016/j.epsl.2004.07.040.

Shackleton, N.J., 2000. The 100,000-year ice-age cycle identified and found to lag temperature, carbon dioxide, and orbital eccentricity. Science 289, 1897–1902.

Singer, B.S., Relle, M.K., Hoffman, K.A., Battle, A., Laj, C., Guillou, H., Carracedo, J.C., 2002. Ar/Ar ages from transitionally magnetized lavas on La Palma, Canary Islands, and the geomagnetic instability timescale. J. Geophys. Res. 107, 2307.

Singer, B.S., Hoffman, K.A., Coe, R.S., Brown, L.L., Jicha, B.R., Pringle, M.S., Chauvin, A., 2005. Structural and temporal requirements for geomagnetic field reversal deduced from lava flows. Nature 434, 633–636.

Suwa, M., 2007. Chronologies for ice cores constrained by their gas records and their implications for climate history for the past 400,000 years, PhD thesis, 189 pp, Princeton University, Princeton.

Suwa, M., Bender, M.L., 2008. Chronology of the Vostok ice core constrained by O_2/N_2 ratios of occluded air, and its implication for the Vostok climate records. Quat. Sci. Rev. 27, 1093–1106.

Tauxe, L., Herbert, T., Shackleton, N.J., Kok, Y.S., 1996. Astronomical calibration of the Matuyama–Brunhes boundary: consequences for magnetic remanence acquisition in marine carbonates and the Asian loess sequences. Earth Planet. Sci. Lett. 140, 133–146.

Valet, J.-P., Meynadier, L., 1993. Geomagnetic field intensity and reversals during the past four million years. Nature 366, 234–238.

Valet, J.-P., Meynadier, L., Guyodo, Y., 2005. Geomagnetic dipole strength and reversal rate over the past two million years. Nature 435, 802–805, doi:10.1038/nature03674.

Wagner, G., Beer, J., Laj, C., Kissel, C., Masarik, J., Muscheler, R., Synal, H.-A., 2000. Chlorine-36 evidence for the Mono Lake event in the Summit GRIP ice core. Earth Planet. Sci. Lett. 181, 1–6.

Wagner, G., Laj, C., Beer, J., Kissel, C., Muscheler, R., Masarik, J., Synal, H.-A., 2001. Reconstruction of the paleoaccumulation rate of central Greenland during the last 75 kyr using the cosmogenic radionuclides ^{36}Cl and ^{10}Be and geomagnetic field intensity data. Earth Planet. Sci. Lett. 193, 515–521.

Yiou, F., Raisbeck, G.M., Baumgartner, S., Beer, J., Hammer, C., Johnsen, S.J., Jouzel, J., Kubik, P.W., Lestringuez, J., Stievenard, M., Suter, M., Yiou, P., 1997. Beryllium 10 in the Greenland ice core project ice core at summit, Greenland. J.Geophys.Res. 102 (C12), 26,783–26,794.